

## A Candidate Brightest Proto-Cluster Galaxy at $z = 3.03$

Jeff Cooke<sup>1, 2</sup>, Elizabeth J. Barton<sup>1</sup>, James S. Bullock<sup>1</sup>, and Kyle R. Stewart<sup>1</sup>

*The Center for Cosmology and the Department of Physics & Astronomy, The University of California, Irvine, Irvine, CA, 92697-4575*

cooke@uci.edu, ebarton@uci.edu, bullock@uci.edu, stewartk@uci.edu

and

Arthur M. Wolfe<sup>1</sup>

*Center for Astrophysics and Space Sciences and the Department of Physics, The University of California, San Diego, La Jolla, CA, 92093-0424*

awolfe@ucsd.edu

### ABSTRACT

We report the discovery of a very bright ( $m_R = 22.2$ ) Lyman break galaxy at  $z = 3.03$  that appears to be a massive system in a late stage of merging. Deep imaging reveals multiple peaks in the brightness profile with angular separations of  $\sim 0.8''$  ( $\sim 25 h^{-1}$  kpc comoving). In addition, high signal-to-noise ratio rest-frame UV spectroscopy shows evidence for  $\sim 5$  components based on stellar photospheric and ISM absorption lines with a velocity dispersion of  $\sigma \sim 460$  km  $s^{-1}$  for the three strongest components. Both the dynamics and high luminosity, as well as our analysis of a  $\Lambda$ CDM numerical simulation, suggest a very massive system with halo mass  $M \sim 10^{13} M_\odot$ . The simulation finds that all halos at  $z = 3$  of this mass contain sub-halos in agreement with the properties of these observed components and that such systems typically evolve into  $M \sim 10^{14} M_\odot$  halos in groups and clusters by  $z = 0$ . This discovery provides a rare opportunity to study the properties and individual components of  $z \sim 3$  systems that are likely to be the progenitors to brightest cluster galaxies.

*Subject headings:* galaxies: high redshift — galaxies: mergers — galaxies: evolution — galaxy clusters: high redshift clusters

---

<sup>1</sup>Visiting Astronomer, W. M. Keck Telescope. The Keck Observatory is a joint facility of the University of California, the California Institute of Technology, and NASA and was made possible by the generous financial support of the W. M. Keck Foundation.

<sup>2</sup>Gary McCue Postdoctoral Fellow

## 1. Introduction

Massive galaxies and galaxy clusters at high redshift provide strong constraints on cosmological models and galaxy formation scenarios. The Lyman break galaxies (LBGs) are a widespread population of high redshift galaxies selected by their rest-frame FUV colors (Steidel et al. 1996, 1998). LBGs at  $z \sim 3$  tend to reside in massive halos  $\langle M_{DM} \rangle \sim 10^{11.5} M_{\odot}$  (Adelberger et al. 2005) and are therefore believed to evolve into present-day massive elliptical galaxies. Although  $\sim 3000$  color-selected  $z > 2$  LBGs have spectroscopic confirmations (e.g. Steidel et al. 2003, 2004; Cooke et al. 2005, 2008), only two systems, selected by their radio emission, have been spectroscopically identified as potential brightest cluster galaxies (Zirm et al. 2005; Miley et al. 2006).

We report the discovery of a bright,  $m_R = 22.2$ , rest-frame FUV color-selected LBG (hereafter LBG-2377) at  $z = 3.03$ . Ground-based imaging and spectroscopy finds no evidence for AGN activity or gravitational lensing making this the most luminous  $z \gtrsim 3$  LBG discovered to date. The deep images and high signal-to-noise ratio (SNR) spectroscopy show evidence for multiple massive components indicative of a system in the late stage of merging. We show that the component velocity dispersion and integrated FUV luminosity suggest that LBG-2377 resides in a very massive halo ( $\sim 10^{13} M_{\odot}$ ) and is likely to evolve into a present-day massive brightest cluster galaxy (§ 3.2). Therefore, LBG-2377 provides a rare opportunity to study the dynamics and properties of a massive LBG halo in the process of formation.

All  $z \gtrsim 3$  LBGs with  $R < 23$  discovered to date are magnified by gravitational lensing. Because all of these show Ly- $\alpha$  in absorption, they are representative of the spectral properties observed in  $\sim 25$ -50% of the LBG population (Shapley et al. 2003). LBG-2377 displays strong Ly- $\alpha$  in emission in two of its components and, because of its brightness, is the only system of its kind. The luminosity of LBG-2377 enables high SNR study of its individual components and thereby a means to constrain the observed range of LBG spectral properties. We briefly describe the imaging and spectroscopic observations of LBG-2377 in §2, highlight the initial analysis of the data in §3, and present a discussion in §4. All magnitudes are in the AB (Fukugita et al. 1996) magnitude system unless otherwise noted and we assume an  $\Omega_M = 0.3$ ,  $\Omega_{\Lambda} = 0.7$  cosmology and use comoving units throughout.

## 2. Observations

### 2.1. Imaging

The deep images of the QSO PC1643+4631A field were obtained on 2001 April 18 using the Low-Resolution Imaging Spectrometer (LRIS; Oke et al. 1995) mounted on the Keck I telescope as part of a multi-field survey for LBGs associated with damped Ly- $\alpha$  systems at  $z \sim 3$  (Cooke et al. 2005). Specifically, the field containing LBG-2377 was imaged in the  $u'BVR_S^1I$  filters with seeing of  $0.7 - 0.9$  arcsec and a depth of  $u' = 28.8$  and  $BVRI \geq 28.1$  ( $1\sigma$ ). We discovered LBG-2377 as an  $R = 22.2$   $z \sim 3$  LBG candidate at R.A. 16:44:48.3, Dec.+46:27:08.2 (J2000.0) toward one edge of the imaged field. The isophotal magnitudes as determined using *SExtractor* (Bertin & Arnouts 1996) source extraction code are:  $u' = 26.5 \pm 0.46$ ,  $B = 24.3 \pm 0.10$ ,  $V = 22.6 \pm 0.03$ ,  $R = 22.2 \pm 0.06$ , and  $I = 22.3 \pm 0.07$ .

LBGs at  $z \sim 3$  have a half-light radius of  $\lesssim 0.''3$  (e.g., Gardner et al. 2001). As illustrated in the contour plot shown in Figure 1, LBG-2377 spans  $\sim 2'' \times 3''$  and has a morphology that can be interpreted as a single extended system exhibiting multiple vigorous star forming regions or multiple separate near-point sources. The ratio of the peaks of the three strongest identified components is approximately 10:5:1 with separations of  $\sim 0.''6 - 1.''0$  ( $\sim 20 - 30h^{-1}$  kpc, comoving). Inspection of the deep images shows that there are no significant lensing-source candidates within  $\sim 10''$ . A potential candidate  $20''$  from LBG-2377 (R.A. 16:44:46.5, Dec +46:27:04.1) does have an effective redshift for lensing ( $z_{phot} = 0.41 \pm 0.2$ ), but would need a halo mass of  $M \gtrsim 7 \times 10^{14} M_\odot$  to provide a significant ( $\gtrsim 2 - 3\times$ ) magnification boost (Minor 2007). Moreover, such a geometry would result in a large distortion of the LBG-2377 image. We see no evidence for this in the deep ground-based images.

### 2.2. Spectroscopy

LBG-2377 was confirmed to be a  $z = 3.03$  galaxy from low-resolution discovery multi-object spectroscopy on 2004 February 18 (Cooke et al. 2005). The data were taken using the 300 line  $\text{mm}^{-1}$  grism on LRIS with a spectral resolution of  $\sim 10\text{\AA}$  FWHM. We acquired follow-up higher resolution, higher SNR longslit spectroscopic observations with LRIS on 21 May 2007 using the 600 line  $\text{mm}^{-1}$  grism blazed at  $4000\text{\AA}$  with the blue arm and the 1200

---

<sup>1</sup> $R_s$  is the H. Spinrad high-throughout night-sky R filter publicly available at the W. M. Keck Observatory. The transformation from Spinrad night-sky  $R_S$  into Johnson VR is  $(R_S - R) = -0.004 - 0.072(V - R) + 0.073(V - R)^2$  (Stern et al. 1999). All  $R_S$  magnitudes presented here have been transformed into the Johnson R bandpass.

line  $\text{mm}^{-1}$  blazed at  $7500 \text{ \AA}$  with the red arm. We used five 1800s exposures in our final combined spectrum that resulted in a SNR of  $10 - 15$  and a resolution of  $\sim 2 - 3 \text{ \AA}$  (Figure 2). Details of the observations will appear in a forthcoming paper.

The spectrum of LBG-2377 is dominated by O and B star continua and displays strong Ly- $\alpha$  emission and little reddening. These features are consistent with the general properties of the  $z \sim 3$  LBG population that display Ly- $\alpha$  in emission (Shapley et al. 2003; Cooke et al. 2005). Although the Ly- $\alpha$  feature appears as a single emission line in the low-resolution discovery spectrum, the higher-resolution high SNR spectroscopy reveals two strong peaks with two possible weak peaks more evident in the individual spectra. The rest-frame FUV shows a complex series of interstellar atomic lines exhibiting gas absorption over velocities  $\gtrsim 2000 \text{ km s}^{-1}$  and evidence for  $\sim 5$  components. Over 20 FUV ISM absorption lines were used to identify and study individual components.

### 3. Analysis

#### 3.1. Components

We identified  $\geq 5$  photospheric lines (to varying confidence levels) of each component to estimate their systemic redshifts. These lines include<sup>2</sup>: SiIII  $\lambda 1294.54, 1296.73, 1417.24$ , CIII  $\lambda 1175.26, 1296.33, 1427.85$  CII  $\lambda 1323.93$ , NIII  $\lambda 1324.32$ , OIV  $\lambda 1343.35$ , and SV  $\lambda 1501.76$ . The strongest components have redshifts  $z = 3.0385, 3.0289$ , and  $3.0244$ . We find a 1-D velocity dispersion of  $\sigma = 460 \text{ km s}^{-1}$  for these three components and  $\sigma = 705 \text{ km s}^{-1}$  for the five components. The details of the identified components are listed in Table 1.

We note that the Ly- $\alpha$  emission and ISM absorption lines of the LBG population show observed velocity offsets of  $\sim +650$  and  $\sim -200 \text{ km sec}^{-1}$  from their systemic velocities, respectively (Pettini et al. 2002; Adelberger et al. 2003; Cooke et al. 2005). The Ly- $\alpha$  and ISM offsets in the identified components are consistent with that of the LBG population. The accepted interpretation is that these offsets are caused by the presence of an expanding galactic-scale shell of gas and dust driven by supernovae and stellar winds. Ly- $\alpha$  photons are largely absorbed in the approaching shell but are resonantly scattered off the receding portion and survive. In this scenario, the two prominent Ly- $\alpha$  peaks observed in the spectrum of LBG-2377 would trace two distinct expanding galactic-scale shells with a systemic velocity difference of  $\sim 550 \text{ km sec}^{-1}$ . Our fit to the components in Table 1 is shown in Figure 3.

---

<sup>2</sup>For consistency with future analyses and because our observations are of similar quality, we use the stellar photospheric values listed in Table 1 of Pettini et al. (2000).

Although the spectra of the components are superposed, the ISM absorption-line strengths and behavior of each component appear internally consistent with being separate systems.

### 3.2. Theoretical expectations

The high luminosity and complex structure of LBG-2377 suggest that this system may be a brightest cluster galaxy in formation. Here we investigate this possibility in the context of  $\Lambda$ CDM. We estimate the dark matter halo mass of LBG-2377 using both its measured kinematics and luminosity. Encouragingly, both estimates suggest a group-scale mass  $\sim 10^{13}M_{\odot}$ . If we assume an NFW halo, our measured  $\sigma \sim 460$  km s $^{-1}$  1-D velocity dispersion corresponds to a halo maximum circular velocity of  $V_{\max} \simeq 1.5\sigma$ , or  $V_{\max} \sim 700$  km s $^{-1}$  (Klypin et al. 1999). At  $z \sim 3$  this implies  $M_{\text{vir}} \sim 10^{13} M_{\odot}$  (e.g. Bullock et al. 2001). Alternatively, if we assume a simple monotonic relationship between galaxy luminosity and dark matter halo  $V_{\max}$  (e.g. Berrier et al. 2006) and use the  $z \sim 3$  LBG luminosity function (Steidel et al. 1999; Sawicki & Thompson 2006), the number density of objects similar to LBG-2377 ( $m_R = 22.2$ ) is  $\sim 10^{-7}$  Mpc $^{-3}h^3$ . This number density corresponds to halos with  $V_{\max} \sim 700$  km s $^{-1}$  at  $z = 3$  (Berrier et al. 2006). The agreement between these two estimates suggests that LBG-2377 does indeed sit within a massive  $V_{\max} \sim 700$  km s $^{-1}$  halo.

Halos that are this massive at  $z = 3$  almost certainly contain substructure. We illustrate this explicitly by examining the high-resolution  $80 h^{-3}$  Mpc $^{-3}$   $\Lambda$ CDM N-body simulation described in Stewart et al. (2007). There are three halos in this box with  $V_{\max} > 600$  km s $^{-1}$  at  $z = 3$  (specifically,  $V_{\max} = 620, 645,$  and  $740$  km sec $^{-1}$ ). These objects have between five and eight  $10^{11}h^{-1}M_{\odot} < M < 10^{12.5}h^{-1}M_{\odot}$  sub-halos within their (physical) virial radii  $R_{\text{vir}} \simeq 90h^{-1}$  kpc  $(M/10^{13}h^{-1}M_{\odot})^{1/3}$ . Note that this substructure mass is typical of that expected for LBG hosts at  $z \sim 3$  ( $\langle M_{\text{LBG}} \rangle \sim 10^{11.5}M_{\odot}$  Adelberger et al. 2005). If we look at simulated halos that are significantly smaller than our estimate, we find that only two out of 16 objects with  $V_{\max} > 450$  km sec $^{-1}$  in the simulation have no sub-halos with  $M > 10^{11}h^{-1}M_{\odot}$ . We conclude that it would be very unlikely for an object like LBG-2377 to exist *without* multiple components.

By following the merger trees of our three  $V_{\max} \gtrsim 600$  km sec $^{-1}$  halos, we find that they evolve from  $M = 10^{13.0-13.5}h^{-1}M_{\odot}$  halos at  $z = 3$  to cluster-mass systems with  $M = 10^{13.9-14.3}h^{-1}M_{\odot}$  at  $z = 0$ . These are among the 12 most massive halos in the box at  $z = 0$  and contain  $\sim 10 - 50$  sub-halos larger than  $10^{11}h^{-1}M_{\odot}$ . This analysis suggests that LBG-2377 will evolve into the dominant galaxy within a large group or cluster by the present day.

### 3.3. Ly- $\alpha$ emission

The double peak nature of the Ly- $\alpha$  feature in LBG-2377 was only detected with higher resolution and SNR. However, multiple Ly- $\alpha$  peaks are not unique to LBG-2377. In the LBG spectroscopic survey of Cooke et al. (2005), we find  $\sim 3\%$  of the low-resolution spectra to display double Ly- $\alpha$  emission peaks and resolved double peaks in their deep image profiles. We can only assume that this fraction increases with higher resolution or SNR. One example of this effect may be found in the sample of Shapley et al. (2006). Of the nine deep high SNR LBG spectra with Ly- $\alpha$  in emission, three have double peaks. Two of the remaining six have redshifts within  $\Delta z = 0.01$  and a separation of  $\sim 2''$  and are consistent with a double-peak system at a larger angular separation. Interestingly, upon inspection of the average internal velocity differences between the Ly- $\alpha$  emission and ISM absorption features ( $\Delta z = z_{em} - z_{abs}$ ), the single peak systems are reported to have  $\langle \Delta z \rangle \sim 550 \text{ km sec}^{-1}$ , whereas the double peak systems have  $\langle \Delta z \rangle \sim 1200 \text{ km sec}^{-1}$ <sup>3</sup>. One plausible interpretation of this discrepancy is the result of the velocity separations, and consequent spectral blending, of two individual interacting systems. Confirming separate components in LBGs showing only Ly- $\alpha$  in absorption is more difficult. However, there are indications of separate components in the intermediate-resolution, high SNR spectrum of MS1512-cB58 (Pettini et al. 2002). The prediction implied is that with higher SNR and/or resolution, a significant fraction, possibly as high as  $\sim 30\%$ , of LBGs with Ly- $\alpha$  in emission have multiple massive components and may indeed be separate interacting or merging systems. This result would be consistent with the fraction of expected major mergers at  $z \sim 3$  from numerical simulations (e.g. Wechsler et al. 2001; Ryan et al. 2007)), and with galaxy formation theories that suggest mergers are an important contributor to the star formation activity in LBGs (Kolatt et al. 1999; Somerville, Primack & Faber 2001).

## 4. Discussion

What is the nature of LBG-2377? Possible interpretations are that LBG-2377 represents either (1) a single extended LBG with  $M \sim 10^{13} M_{\odot}$  exhibiting multiple regions of vigorous star formation, (2) a single, extended LBG with mass more typical of LBGs ( $M \sim 10^{12} M_{\odot}$ ) that appears over-luminous due to exceptionally high bursts of star formation, (3) multiple

---

<sup>3</sup>This value omits the system C32 that shows a higher redshift for absorption than emission for one of the two components. Including this system results in a  $\Delta z \sim 900 \text{ km sec}^{-1}$ . If the absorption features of the lower redshift systems are weak or narrow in this interpretation, adopting a typical  $\Delta z$  for the that system would result in  $\Delta z \sim 1100 \text{ km sec}^{-1}$  for the assumed two components.

unbound  $M \sim 10^{12}M_{\odot}$  LBGs in near proximity, or (4) multiple LBGs in a  $M \sim 10^{13}M_{\odot}$  halo observed in a late stage of merging. We discuss each scenario below and show that the evidence gathered to date favors interpretation 4.

If the component stellar photospheric lines are misidentified and the complex nature of the ISM absorption and Ly- $\alpha$  emission lines are ascribed to violent mixing of the ISM and discrete star forming regions separated by  $\geq 25h^{-1}$  kpc, interpretation 1 may hold. However, a single  $M \sim 10^{13}M_{\odot}$  halo with no massive sub-halos is in conflict with simulation results. In this interpretation, LBG-2377 is indeed a massive and extended system that appears to be experiencing a monolithic burst of star formation. Under interpretation 2, LBG-2377 would be in less conflict with simulations yet the above assumptions for stellar and ISM lines must hold. In this case, LBG-2377 is a single system undergoing an unusually strong star formation episode at a level that has not been witnessed in any other LBG. In addition, this exceptional star formation must be occurring in multiple regions separated by  $\geq 25h^{-1}$  kpc. If the velocity offsets are interpreted as redshifts, as in interpretation 3, the systems would have separations of  $\sim 5h^{-1}$  Mpc comoving. An event of three or more unbound systems with  $M \sim 10^{12}M_{\odot}$ ,  $\leq 1.''0$  angular separations, and an LBG density of  $\sim 10^{-3} - 10^{-4}h^3$  Mpc $^{-3}$  has a vanishingly low probability, even if the systems were given reasonable peculiar velocities. The most likely scenario is interpretation 4 because it is consistent with the extended nature and multiple peaks seen in the images, the superposed spectra of multiple identified components, the observed velocity dispersion, and the expectations from the simulation. In addition, this interpretation provides a natural driver for the observed star formation and bright integrated luminosity. Furthermore, the double Ly- $\alpha$  emission peak of LBG-2377 is also seen in other LBGs which exhibit two distinct components in their deep images and Ly- $\alpha$  emission-line velocity differences consistent with close galaxy pairs.

LBG-2377 is a fortuitous discovery that enables detailed study of the individual components of a candidate massive galaxy in the late stage of merging. Study of the relationships between the spectral and spatial properties of this single system will constrain the formation processes of the LBG population and lend insight into the fraction of LBGs detected as a result of merger induced star formation. Future high-resolution ground-based IFU data on existing instruments, such as OSIRIS on Keck, have the capability to resolve the velocity structure of LBG-2377 and hence its true nature.

J.C. is supported in part by a Gary McCue postdoctoral fellowship through the Center for Cosmology at the University of California, Irvine. E.J.B. and J.S.B. are supported by the Center for Cosmology at the University of California, Irvine and J.S.B. and K.S. are supported by NSF grant AST-0507816. The authors wish to recognize and acknowledge the very significant cultural role and reverence that the summit of Mauna Kea has always had

within the indigenous Hawaiian community. We are most fortunate to have the opportunity to conduct observations from this mountain.

## REFERENCES

- Adelberger, K. L., Steidel, C. C., Shapley, A. E., & Pettini, M. 2003, *ApJ*, 584, 45
- Adelberger, K. L., Steidel, C. C., Pettini, M., Shapley, A. E., Reddy, N. A., & Erb, D. K. 2005, *ApJ*, 619, 697
- Berrier, J., Bullock, J. S., Zentner, A. R., Guenther, H., Barton, E. J., Kravtsov, A. V., & Wechsler, R. H. 2006, *ApJ*, 652, 56
- Bertin, E. & Arnouts, S. 1996, *A&AS*, 117, 393
- Bullock, J. S., Kolatt, T. S., Sigad, Y., Somerville, R. S., Kravtsov, A. V., Klypin, A. A., Primack, J. R., & Dekel, A. 2001, *MNRAS*, 321, 559
- Cooke, J., Wolfe, A. M., Gawiser, E., & Prochaska, J. X. 2005, *ApJ*, 621, 596
- Cooke, J., Barton, E., Barbour, E. Gawiser, E., & Wolfe, A. 2008 in preparation
- Fukugita, M., Ichikawa, T., Gunn, J. E., Doi, M., Shimasaku, K., & Schneider, D. P. 1996, *AJ*, 111, 1748
- Gardner, J. P., Brown, T. M., & Ferguson, H. C. 2000, *ApJ*, 542L, 79
- Klypin, A.; Gottlber, S., Kravtsov, A. V., & Khokhlov, A. M. 1999, *ApJ*, 516, 530
- Kolatt, T. S., Bullock, J. S., Somerville, R. S., Sigad, Y., Jonsson, P., Kravtsov, A. V., Klypin, A. A., Primack, J. R., Faber, S. M., & Dekel, A. 1999, *ApJ*, 523, 109
- Law, D. R., Steidel, C. C., Erb, D. K., Pettini, M., Reddy, N. A., Shapley, A. E., Adelberger, K. L., & Simenc, D. J. 2007, *ApJ*, 656, 1
- Miley, George K., Overzier, Roderik A., Zirm, Andrew W., Ford, Holland C., Kurk, Jaron, Pentericci, Laura, Blakeslee, John P., Franx, Marijn, Illingworth, Garth D., Postman, Marc, Rosati, Piero, Röttgering, Huub J. A., Venemans, Bram P., & Helder, Eveline 2006, *ApJ*, 650, 29
- Minor, Q. 2007, private communication.

- Oke, J. B., Cohen, J. G., Carr, M., Cromer, J., Dingizian, A., Harris, F. H., Labrecque, S., Lucinio, R., Schaal, W., Epps, H., & Miller, J. 1995, *PASP*, 107, 375
- Pettini, M., Steidel, C. C., Adelberger, K. L., Dickinson, M., & Giavalisco, M. 2000, *ApJ*, 528, 96
- Pettini, M., Rix, S. A., Steidel, C. C., Adelberger, K. L., Hunt, M. P., & Shapley, A. E. 2002, *ApJ*, 569, 742
- Ryan, R. E., Cohen, S. H., Windhorst, R. A., & Silk, J. 2007, arXiv:0712.0416
- Sawicki, M. & Thompson, D. 2006, *ApJ*, 642, 653
- Shapley, A. E., Steidel, C. C., Adelberger, K. L., & Pettini, M. 2003, *ApJ*, 588, 65
- Shapley, A. E., Steidel, C. C., Pettini, M., Adelberger, K. L., & Erb, D. K. 2006, *ApJ*, 651, 688
- Somerville, R. S., Primack, J. R., & Faber, S. M. 2001 *MNRAS*, 320, 504
- Steidel, C. C., Giavalisco, M., Pettini, M., Dickinson, M., & Adelberger, K. L. 1996, *ApJ*, 462, 17
- Steidel, C. C., Adelberger, K. L., Giavalisco, M., Dickinson, M., Pettini, M., & Kellogg, M. 1998, *ApJ*, 492, 428
- Steidel, C. C., Adelberger, K. L., Giavalisco, M., Dickinson, M., & Pettini, M. 1999, *ApJ*, 519, 1
- Steidel, C. C., Adelberger, K. L., Shapley, A. E., Pettini, M., Dickinson, M., & Giavalisco, M. 2003, *ApJ*, 592, 728
- Steidel, C. C., Shapley, A. E., Pettini, M., Adelberger, K. L., Erb, D. K., Reddy, N. A., & Hunt, M. P. 2004, *ApJ*, 604, 534
- Stern, D., Dey, A., Spinrad, H., Maxfield, L., Dickinson, M., Schlegel, D., & Gonzalez, R. A. 1999, *AJ*, 117, 1122
- Stewart, K. R., Bullock, J. S., Wechsler, R. H., Maller, A. H., & Zentner, A. R. 2007, arXiv:0711.5027
- Wechsler, R. H., Somerville, R. S., Bullock, J. S., Kolatt, T. S., Primack, J. R., Blumenthal, G. R., & Dekel, A. 2001, *ApJ*, 554, 85

Zirm, A. W., Overzier, R. A., Miley, G. K., Blakeslee, J. P., Clampin, M., De Breuck, C., Demarco, R., Ford, H. C., Hartig, G. F., Homeier, N., Illingworth, G. D., Martel, A. R., Röttgering, H. J. A., Venemans, B., Ardila, D. R., Bartko, F., Benítez, N., Bouwens, R. J., Bradley, L. D., Broadhurst, T. J., Brown, R. A., Burrows, C. J., Cheng, E. S., Cross, N. J. G., Feldman, P. D., Franx, M., Golimowski, D. A., Goto, T., Gronwall, C., Holden, B., Infante, L., Kimble, R. A., Krist, J. E., Lesser, M. P., Mei, S., Menanteau, F., Meurer, G. R., Motta, V., Postman, M., Rosati, P., Sirianni, M., Sparks, W. B., Tran, H. D., Tsvetanov, Z. I., White, R. L., & Zheng, W. 2005, *ApJ*, 630, 68

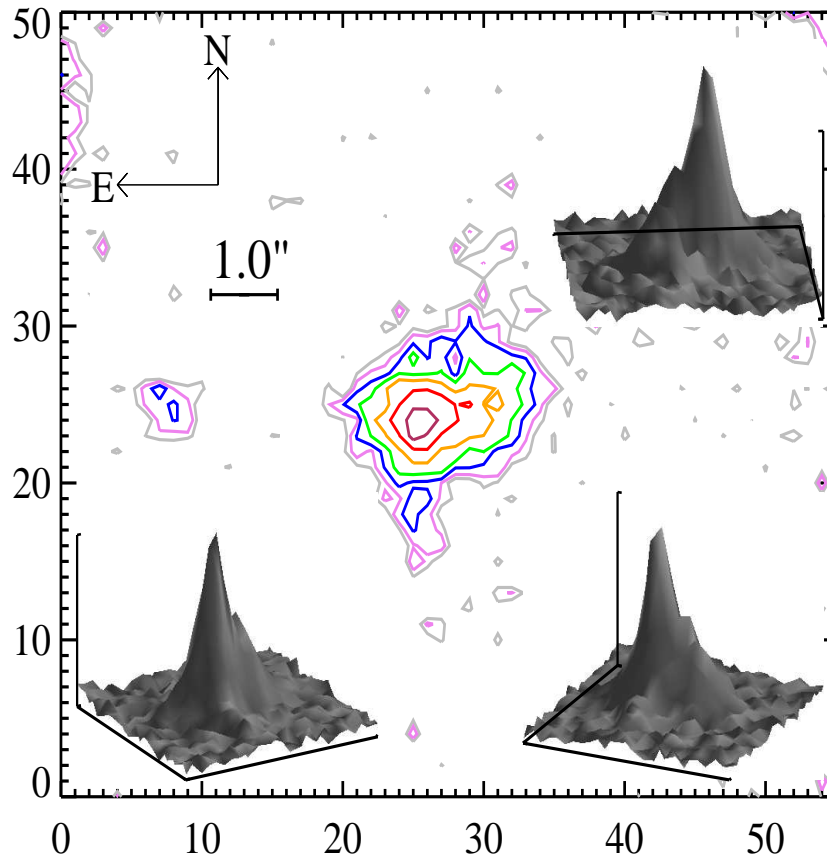


Fig. 1.— Contour plots of LBG-2377. The 2-D plot indicates a primary peak located slightly to the E of the object centroid. Secondary and tertiary peaks are detected W and SE of the centroid, respectively. Three 3-D contour plots are inset with rotations (clockwise from upper-right),  $185^\circ$ ,  $335^\circ$ , and  $30^\circ$  ( $S=0^\circ$ ).

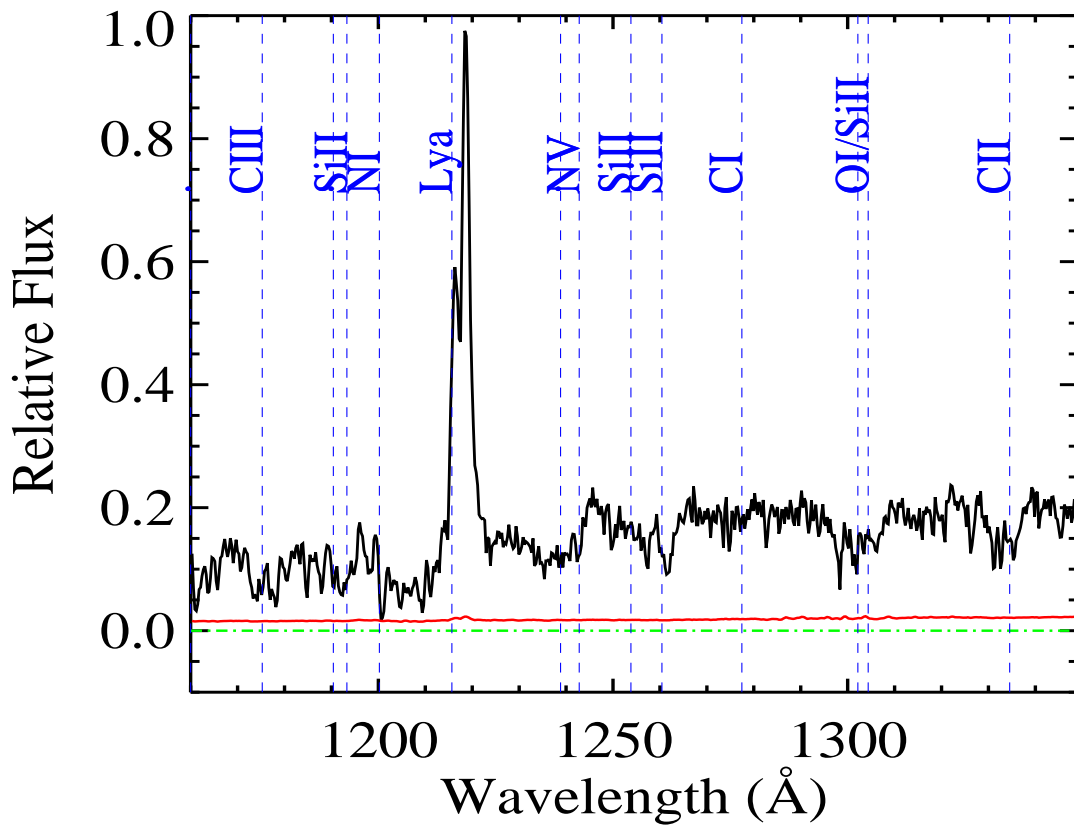


Fig. 2.— Spectrum of LBG-2377. This section is shown to illustrate both the double-peak Ly- $\alpha$  emission feature and broad, complex interstellar absorption features [vertical (*blue*) dashed lines]. In all spectra in this paper, the green line indicates zero flux and the red line is the error array.

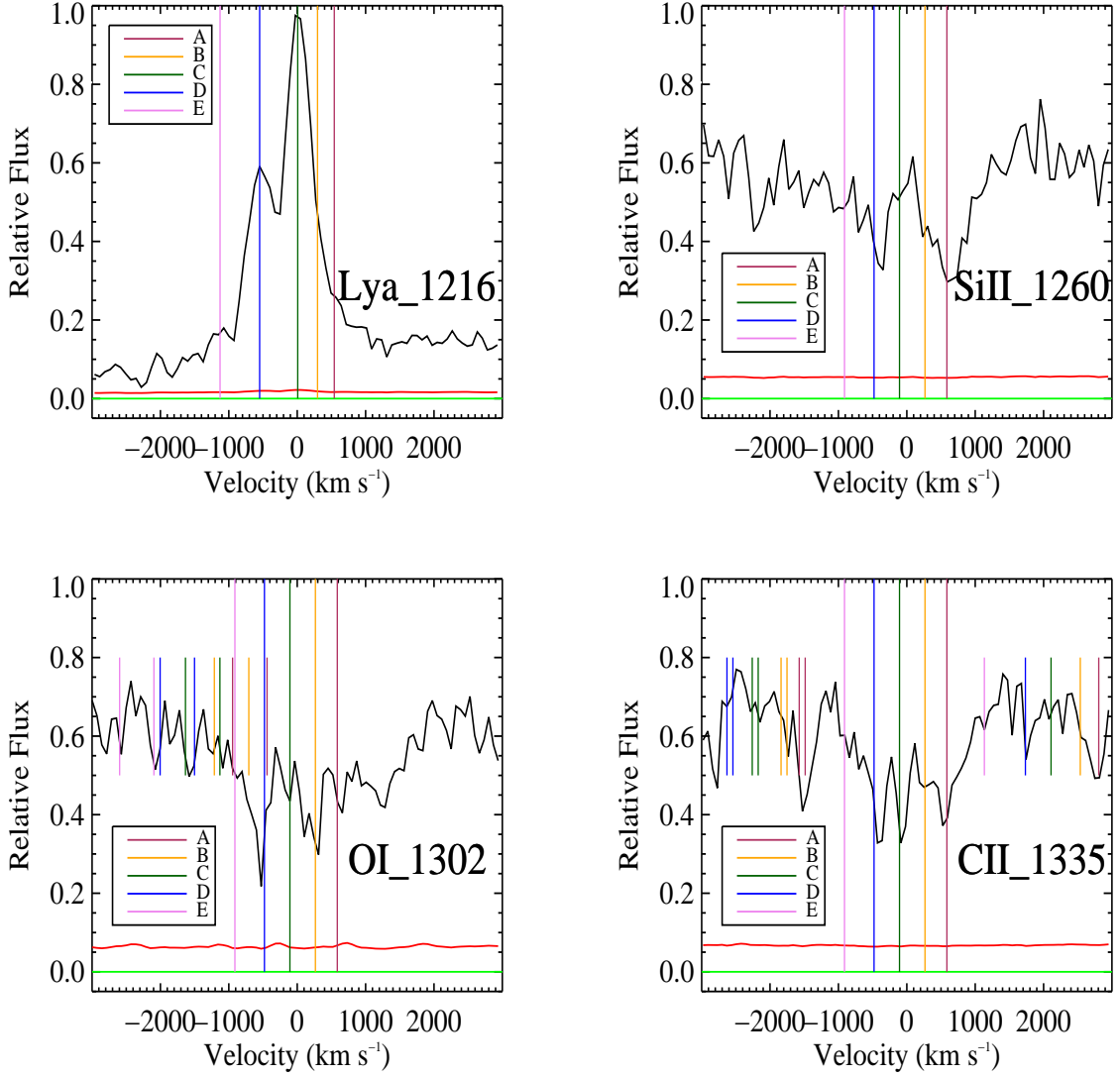


Fig. 3.— Spectrum of LBG-2377 showing five tentative components (A - E in Table 1) identified using 21 ISM features. Velocities are with respect to the average of components A, C, & D. *Upper left:* The two strong Ly- $\alpha$  emission lines (components C & D) and three potential weak Ly- $\alpha$  lines [A, B, & E]. *Clockwise from the upper right:* Fits for the ISM transitions SiII, CII, and OI. Also shown are the stellar photospheric features SiIII 1294.5, 1296.7, CIII 1296.3, CII 1323.9, NIII 1324.3, and OIV 1343.4 (not labeled for clarity) indicated by short vertical lines. The signal-to-noise ratio is  $\sim 15$  in these regions, therefore the more prominent features are real. Each absorption feature is in agreement with their respective systemic redshift to within the spectral resolution ( $\sim 150 \text{ km sec}^{-1}$ ).

Table 1. LBG-2377 Components

Comp.	$z_{Phot}$	$z_{ISM}^a$	$z_{Ly\alpha}$	$\Delta v_{ISM}^{a\ b}$	$\Delta v_{Ly\alpha}^b$
A	3.0385	3.0354	(3.0488) <sup>c</sup>	-230	(765) <sup>c</sup>
B	3.0343	3.0308	...	-260	...
C	3.0289	3.0258	3.0416	-230	945
D	3.0244	3.0209	3.0341	-260	725
E	(3.0161) <sup>c</sup>	(3.0143) <sup>c</sup>	(3.0263) <sup>c</sup>	(-135) <sup>c</sup>	(760) <sup>c</sup>

<sup>a</sup>Averaged fit to multiple features.

<sup>b</sup>Approximate velocity offset with respect to the stellar photospheric velocities in  $\text{km sec}^{-1}$ .

<sup>c</sup>Features are weak and respective values have a lower confidence level.